EXAFS investigation of nanoparticles produced in a thermal plasma process

Dirk Lützenkirchen-Hecht[a], Peter Buchner[b], Jürgen Uhlenbusch[b], Hans-Henning Strehblow[c] and Ronald Frahm[a]

[a]*Institut für Angewandte Physik, Heinrich-Heine-Universität Düsseldorf, Universitätsstr.1, 40225 Düsseldorf, Germany,*
[b]*Institut für Laser- und Plasmaphysik, Heinrich-Heine-Universität Düsseldorf, Universitätsstr.1, 40225 Düsseldorf, Germany, and*
[c]*Institut für Physikalische Chemie und Elektrochemie, Heinrich-Heine-Universität Düsseldorf, Universitätsstr.1, 40225 Düsseldorf, Germany.*
Email: hechtd@uni-duesseldorf.de

Nanosized ceramic powders (Cu/SiC, Y_2O_3-stabilized cubic ZrO_2) were produced by evaporation of coarsely grained powders of the respective materials in an inductively coupled thermal plasma process and rapid quenching of the vapor. The atomic short range order of these nanoparticles with an average diameter of about 10 nm was investigated ex situ with EXAFS. The results are compared to crystalline reference materials.

Keywords: **Nanosized materials, Fe, Cu, Cu/SiC, Y_2O_3-stabilized ZrO_2**

1. Introduction

Nanosized particles are of growing interest for materials science and industrial applications due to their promising mechanical, chemical and electrical properties (e.g. Siegel (1994)). In addition, applications in catalysis and electrochemical engineering have been discussed. Up to date, a wide spectrum of nanosized metal powders such as metallic Ni, Fe and Cu, and ceramic SiC- or Cu/SiC-compounds have been synthesized by inductively coupled thermal plasma processes (Kong and Lau (1990)). Due to its inherent sensitivity to short range order structures, EXAFS was successfully applied for the investigation of nanosized materials such as clusters (see e.g.Yokoyama *et. al.* (1989), Cimini and Prins (1997), Kakar *et al.* (1997)). In this contribution, we report on EXAFS investigations of nanosized Cu/SiC and Y_2O_3-stabilized ZrO_2 particles which were produced by evaporation of coarse grained powders (10 μm grain size) of the respective materials in an inductively coupled plasma process and rapid quenching of the vapor.

2. Experimental details

Particles were synthesized in a plasma reactor which mainly consists of a radio frequency generator (frequency: 3.5 MHz, max. rf power: 35 kW), a quartz plasma torch, a quench chamber and a filter system. The inductively coupled plasma is burning in pure argon (99.999% purity) at pressure conditions of typically 400-800 hPa. The precursor materials (typically 10 μm maximum particle size) were fed both axially through the plasma and radially into the tail flame. Addition of N_2 gas (99.999% purity) in the tail flame region results in rapid quenching of the evaporated material and the formation of nanosized particles. The resulting powders were collected in a combination of an electrostatic filter and a metal mesh filter. Details of the particle preparation are given elsewhere (Buchner (1998)). Spectroscopic measurements of the plasma and numerical modeling both indicate temperatures of approx. 10000 K in the hot plasma zone (Buchner *et. al.* (1997)). This temperature is sufficient for the complete evaporation of powders up to a particle size of 15 μm for the present plasma conditions according to model calculations (Buchner et. al. (1997)).

The synthesized particles were characterized by X-ray diffraction (XRD), transmission electron microscopy (TEM) and X-ray photoelectron spectroscopy (XPS). According to TEM investigations, a mean particle size of about (10 ± 2.5) nm was observed for the Cu/SiC particles while a large fraction of the Y_2O_3-stabilized ZrO_2 powder consists of agglomerated particles with ≈5 nm diameter. In addition, however, a small number of larger particles of about 40 nm size were found in this material. XRD results agree quantitatively with this observation (Buchner (1998)). These investigations also show that most of the synthesized nano-powders reveal crystalline structures. However, weak Bragg intensities, peak broadening and an increasing diffuse scattered background suggests the presence of disordered contributions.

The EXAFS experiments described here were performed at the RÖMO II beamline at the DORIS III storage ring at HASYLAB (Frahm (1989)). Transmission EXAFS data were collected in the vicinity of the Y and Zr K-edges at 17038.4 eV and 17997.6 eV and of the Cu K-edge at 8978.9 eV, respectively. The intensities of the incident and the transmitted beam were monitored by N_2 or Ar filled ionization chambers. A reference foil was measured simultaneously with each sample for energy calibration. We used a double crystal monochromator equipped with two pairs of flat Si(111) and Si(311) crystals. Cu- and Zr-metal foils, Cu_2O, CuO and $CuCO_3$ as well as the corresponding powders which were used as base material for the plasma process were investigated for comparison to the nanoparticles.

3. Results and Discussion

In Fig. 1, EXAFS spectra covering the K-edges of Y at 17038 eV and Zr at 17998 eV are presented for a precursor material and a plasma synthesized Y_2O_3-ZrO_2 powder. Obviously, both spectra are very similar. Especially the ratio of the edge height of the Zr and the Y edges are identical. We found an Y/Zr ratio of 0.262 ± 0.013 for the precursor materials (four samples) and of 0.254 ± 0.015 for the ultra fine powders (seven samples), respectively. Therefore the plasma synthesized Y_2O_3-ZrO_2-samples have the same content of Zr and Y compared to the precursor material. The k^3-weighted fine structures $\chi_{Zr}(k)*k^3$ extracted above the Zr K-edge of both materials are compared in the upper insert of Fig. 1. Both samples yield very similar results, i.e. the atomic short range order structure of the plasma synthesized Y_2O_3-ZrO_2 nanoparticles is very similar to that of the polycrystalline precursor material which is used for the plasma process. However, the fine structure from the crystalline precursor material (dashed line) reveals larger amplitudes compared to the

nanosized material (full line), especially for higher k values (k ≥ 6 Å⁻¹). This is due to a slightly increased disorder in the nanosized Zr-oxide compound. Also, the Fourier transforms of the extracted fine structures reveal the similarity of the short range order structure of the nanosized powder and the precursor material, as can be seen in the lower insert of Fig. 1. In addition, the Fourier transforms of the absorption spectra presented here give no evidence for metallic Zr as can be seen by the absence of the metallic Zr-Zr coordination at about 2.9 Å (dashed vertical line in the lower insert of Fig. 1).
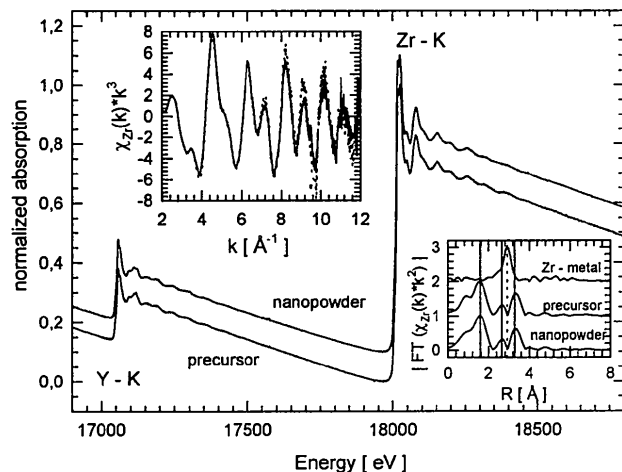

Figure 1
Normalized X-ray absorption spectra of a plasma synthesized Y_2O_3-ZrO_2 powder and the polycrystalline precursor material in the vicinity of the Y and Zr K-edges (spectra are shifted vertically with respect to each other). Upper insert: k^3-weighted fine structures $\chi_{Zr}(k)*k^3$ extracted above the Zr K-edge of both samples. Full line: nanopowder sample, dotted line: polycrystalline precursor material. Lower insert: Magnitude of the Fourier transforms of the k^2-weighted fine structures $\chi_{Zr}(k)*k^2$ (k-range from 2 Å⁻¹ to 11.9 Å⁻¹, data not phase shift corrected). For comparison, the FT of a Zr metal foil is also presented. Peak positions of the Zr-O and Zr-Zr coordinations of the oxide and the Zr-Zr coordination of Zr-metal are indicated by full and dashed vertical lines, respectively.

For a more detailed analysis of the measured data, the peaks representing the first Zr-O and Zr-Zr coordinations at about ≈1.6 Å and ≈3.2 Å radial distance were isolated by means of filter functions, back-transformed into k-space and fitted with phases and amplitudes calculated by FEFF (Rehr et. al. (1992)). The fits were performed both for k^1- and k^3-weighted data. Mean values for the determined bond distances R_i, coordination numbers N_i and the disorder σ_i are given in table 1 for the nanosized ZrO_2 powder as well as for the precursor material, respectively. For comparison, the distances and coordination numbers calculated from the crystallographic structure of cubic ZrO_2 (fluorite structure, (Wyckoff, 1963)) are also given. In general, the bond distances determined from the EXAFS data (R_1≈2.13 Å, R_2≈3.56 Å) are smaller than the crystallographic data for both shells (R_1≈2.195 Å, R_2≈3.585 Å). Although the coordination number for the first shell N_1≈7.1 is comparable to the value which is expected for the monoclinic baddeleyite ZrO_2-structure (N_1=7) and significantly smaller than the coordination number of cubic ZrO_2 (N_1=8), the existance of the baddeleyite ZrO_2-phase is not very likely. The results of our XRD-analysis clearly demonstrated the presence of the cubic phase for the plasma synthesized powder as well as for the precursor material.

In addition, the coordination number obtained for the second shell (Zr-Zr coordination) N_2≈12 can be anticipated for cubic ZrO_2, while for the baddeleyite ZrO_2-phase a value of about 6 is expected.

Table 1
EXAFS results for the first Zr-O and Zr-Zr coordinations of nanosized ZrO_2 powders prepared in a thermal plasma process and the corresponding polycrystalline precursor material. Coordination numbers and radii calculated from the crystallographic structure are given for comparison.

coordination		Plasma synthesized nano powder	Precursor material	Crystallographic data (cubic ZrO_2)
	R_1 / Å	2.138 ± 0.005	2.124 ± 0.002	2.195
Zr – O	N_1	7.15 ± 0.28	7.02 ± 0.16	8
	σ_1 / Å	0.091 ± 0.002	0.084 ± 0.002	--
	R_2 / Å	3.542 ± 0.004	3.572 ± 0.004	3.585
Zr – Zr	N_2	11.67 ± 0.13	12.61 ± 0.30	12
	σ_2 / Å	0.105 ± 0.002	0.100 ± 0.001	--

The results of our EXAFS data analysis suggests that the disorder in the plasma synthesized ZrO_2 powders is slightly enhanced compared to the polycrystalline precursor material; i.e. values of σ_1≈0.091 Å and σ_2≈0.105 Å were determined for the first two shells of the nanopowder, while the corresponding values are σ_1≈0.084 Å and σ_2≈0.100 Å for the ZrO_2 precursor. These small differences could be a result of the strong correlation between N and σ in the fit procedure, however, larger values for the coordination number and smaller values for the Debye-Waller factor were found for the second Zr-Zr coordination shell, while for the first Zr-O coordination, N_1 is practically identical for the precursor material and the nanosized powder and only a larger σ_1 value was found for the plasmasynthesized material. Therefore, the a slightly enhanced disorder compared to the polycrystalline reference material is present in the nanosized powder.

In Fig. 2(a), normalized Fourier transforms calculated from absorption spectra of several plasma synthesized Cu/SiC-samples (50% molar content SiC), the Cu/SiC precursor material and Cu reference compounds are depicted. While the precursor material clearly reveals the atomic short range order of metallic copper with the intense Cu-Cu nearest neighbor peak at about 2.3 Å radial distance and also the 2nd, 3rd and 4th nearest neighbor coordination peaks between ca. 3 Å and 5 Å, strong peaks at about 1.3 Å dominate the FTs of the plasma synthesized powders. These peaks are belonging to Cu-O coordinations. In addition, only a weak Cu-Cu peak is detected at about 2.3 Å. The presence of $CuCO_3$ is not very likely due to the absence of its prominent peak at ≈3.2 Å. Therefore, the copper fraction of the nanosized Cu/SiC powders seems to be a composition of metallic Cu and Cu-oxides (Cu_2O and CuO), in agreement with XRD experiments (Buchner (1998)).

In contrast to the ZrO_2-powders, however, a straightforward EXAFS data analysis cannot be performed since the nanosized Cu-SiC powders always represent a mixture of several different Cu-compounds; i.e. the separation of the different contributions is necessary in order to extract more detailed near range order structural information.

For a first simple analysis, the magnitude of the 2nd and 3rd nearest neighbor coordination peaks in the FT's of the nanosized powders were compared to those of the related reference compounds. Obviously, the crystalline reference materials reveal larger peaks at about 3 Å radial distance. This can be seen more clearly in Fig. 2(b), where simulated FT's of several Cu/Cu-oxide mixtures are presented. These calculations were performed using the absorption spectra of crystalline Cu, Cu$_2$O and CuO with different fractions of the metal and the oxides. The ratio between Cu metal and the oxidic fraction was chosen so that the intensity ratio of the first Cu-O coordination of the oxides at about 1.3 Å and the first Cu-Cu coordination at ca. 2.3 Å was reproduced by the calculations. As a first result, the calculations suggest that the metal fraction in the plasmasynthesized Cu/SiC nanopowders is only about 10-20%, while the oxidic fraction is the dominant component.
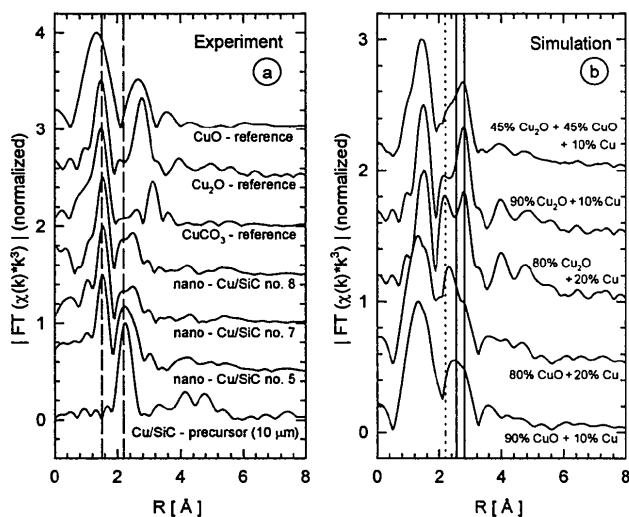
particles is very similar to the polycrystalline precursor material, with only a slightly increased disorder. In contrast, strong oxidic contributions and only weak Cu metal signals were found for the Cu/SiC nanoparticles. In addition, this oxidic fraction seems to be highly disordered compared to the crystalline reference materials.

References:

Buchner, P., Ferfers, H., Schubert, H. and Uhlenbusch, J. (1997).*Plasma Sources Sci. and Technol.* **6**, 450 – 459.
Buchner, P. (1998). PhD-Thesis, Heinrich-Heine-Universität Düsseldorf.
Cimini, F. and Prins, R. (1997). *J. Phys. Chem. B* **101**, 5277 - 5284.
Frahm, R. (1989). *Rev. Sci. Instrum.* **60**, 2515 – 2518.
Kakar, S., Björneholm, O., Weigelt, J., de Castro, A.R.B., Tröger, L., Frahm, R., Möller, T., Knop, A. and Rühl, E. (1997). *Phys. Rev. Lett.* **78**, 1675 - 1678.
Kong, P.C. and Lau, Y.C. (1990). *Pure & Applied Chem.* **62**, 1809 - 1816.
Rehr, J.J., Albers, R.C. and Zabinsky, Z.I. (1992). *Phys. Rev. Lett.* **69**, 3397 - 3400.
Siegel, R. (1994). *Encyclopedia of Applied Physics* **11**, 173 – 200.
Wyckoff, R.W.G. (1963). *Crystal Structures, 2nd Ed. Vol. 1*, Interscience Publishers, pp. 239.
Yokoyama, T., Kimoto, S. and Ohta, T. (1989).*Jap. J. Appl. Phys.* **28**, L851 – L853.

Figure 2
(a) Normalized magnitude of the Fourier transform of the k^3-weighted fine structures χ(k)*k^3 of several plasma synthesized Cu/SiC nanopowders (k-range from 2 Å^{-1} to 11.5 Å^{-1}, data not phase shift corrected). For comparison, the FT's of a Cu metal foil, polycrystalline Cu$_2$O, CuO and CuCO$_3$ powders are also presented. Peaks corresponding to the first Cu-O coordinations of the oxides and the Cu-Cu peak of Cu metal are indicated by dashed vertical lines. (b) Calculated Fourier transforms for some hypothetical mixtures of Cu-metal with different amounts of Cu$_2$O and CuO. Peak positions of the Cu-Cu coordination of the oxides (full lines) and Cu-metal (dotted line) are indicated.

In addition, the comparison of the calculated and the measured FTs shows that the intensity of the second Cu-Cu coordination of the oxides at about 3 Å (full vertical lines in Fig. 2(b)) is significantly larger for the calculated FTs. This observation suggests that the near range order of the oxidic fraction is not fully developed for the Cu/SiC nanoparticles; i.e. the disorder is enhanced compared to the polycrystalline reference materials.

4. Conclusions

EXAFS investigations of Cu / SiC and Y$_2$O$_3$-ZrO$_2$ nanoparticles synthesized in a thermal plasma process were performed. The results show that the short range order structure of the Y$_2$O$_3$-ZrO$_2$